

## Theoretical Analysis of Neutron Double-Differential Cross Section of $n+^{10}\text{B}$ at 14.2 MeV

ZHANG Jing-Shang

China Institute of Atomic Energy, P.O. Box 275(41), Beijing 102413, China

(Received August 2, 2002)

**Abstract** *By using a new reaction model for light nuclei, the double-differential cross sections of  $n+^{10}\text{B}$  reactions at  $E_n = 14.2$  MeV have been analyzed. In the case of  $n+^{10}\text{B}$  reactions there are over one hundred opened partial reaction channels. Besides the sequential particle emissions, there is also the three-body breakup process, in which the kinematics is classified into four types. In this paper the opened reaction channels are listed in detail with the LUNF code, with which the model calculation is performed to analyze the total outgoing neutron double-differential cross sections. All of the fittings agree fairly well with the measurements. The calculation results indicate that the pre-equilibrium mechanism dominates the whole reaction processes, and the recoil effect in light nuclear reaction is essentially important.*

**PACS numbers:** 25.10.+s

**Key words:** light nucleus reaction, double-differential cross sections

### 1 Introduction

Being very large neutron absorption cross section at low energies,  $^{10}\text{B}$  has long been selected as the shielding material in nuclear engineering. In the reactions of  $n+^{10}\text{B}$  there are many partial reaction channels to be opened even at incident neutron energies of 14 MeV. Since the new approach for description of neutron induced light nucleus reaction was proposed in 1999,<sup>[1]</sup> many experimental data, especially on the double-differential measurements, have been analyzed. The key point is that the angular momentum conservation in pre-equilibrium emission mechanism from a compound nucleus to the discrete levels of the residual nuclei is taken into account properly.<sup>[2]</sup> Meanwhile, the energy balance for variety particle emissions could be obtained by the accurate kinematics.

Only one double-differential measurement of the total outgoing neutrons for  $n+^{10}\text{B}$  was measured by M. Baba *et al.*, at  $E_n = 14.2$  MeV in 1985,<sup>[3]</sup> which has been analyzed with this new approach in this paper.

In the case of  $E_n < 20$  MeV, in terms of the fitting the measured data, including the total cross section, elastic scattering, non-elastic cross section, elastic scattering angular distribution, and the energy-angular spectra of outgoing neutrons, the optical potential parameters have been obtained.

In Sec. 2 the reaction channels of  $n+^{10}\text{B}$  are listed in detail. It turns out that the different levels of the residual nucleus reached by sequential particle emissions could belong to different reaction channels, due to the different decay modes from these levels. The illustration on this respect is given in this section as more as distinct. Although there is a large number of the partial reaction channels, the research indicates that the representation of the double-differential cross sections can be presented in four types according to their kinematics, which is given in Sec. 3.

As the calculations performed for other light nuclei, the broadening effect must be taken into account in the

fitting procedure. Meanwhile, the transformation from CMS to LS is needed in the fitting procedure. The related formulation of the broadening expansions and the motion system transformation can be found in Secs. 5 and 6 of Ref. [1].

The calculated energy-angular spectra of the outgoing neutrons at  $E_n = 14.2$  MeV are shown in Figs. 1 ~ 10 in Sec. 4. The calculated results of the outgoing neutrons agree very well with the experimental data. A summary is given in Sec. 5.

### 2 Reaction Channels

In view of the  $n+^{10}\text{B}$  reactions with  $E_n < 14$  MeV, the opened reaction channels and their reaction  $Q$ -values are listed as follows:

$$n + ^{10}\text{B} = \left\{ \begin{array}{ll} \gamma + ^{11}\text{B} & Q = 11.453 \text{ MeV}, \\ n' + ^{10}\text{B} & Q = 0.000 \text{ MeV}, \\ p + ^{10}\text{Be} & Q = 0.225 \text{ MeV}, \\ \alpha + ^7\text{Li} & Q = 2.790 \text{ MeV}, \\ ^5\text{He} + ^6\text{Li} & Q = -5.354 \text{ MeV}, \\ d + ^9\text{Be} & Q = -4.620 \text{ MeV}, \\ t + ^8\text{Be} & Q = 0.230 \text{ MeV}, \\ 2n + ^9\text{B} & Q = -8.436 \text{ MeV}, \\ np + ^9\text{Be} & Q = -6.586 \text{ MeV}, \\ n\alpha + ^6\text{Li} & Q = -4.459 \text{ MeV}, \\ nd + ^8\text{Be} & Q = -6.027 \text{ MeV}, \\ pn + ^9\text{Be} & Q = -6.586 \text{ MeV}, \\ p\alpha + ^6\text{He} & Q = -7.184 \text{ MeV}, \\ \alpha n + ^6\text{Li} & Q = -4.459 \text{ MeV}, \\ \alpha p + ^6\text{He} & Q = -7.184 \text{ MeV}, \\ 2\alpha + t & Q = -0.323 \text{ MeV}, \\ dn + ^8\text{Be} & Q = -6.027 \text{ MeV}. \end{array} \right.$$

The threshold energies of all reaction channels are less than 10 MeV, so all of them are opened at 14.2 MeV.

The residual nucleus  ${}^9\text{B}$  from two neutron emissions' process is unstable, all of the levels of  ${}^9\text{B}$  can emit proton or  $\alpha$ -particle. Consequently,  ${}^9\text{B}$  decays into one proton and two  $\alpha$ -particles. Hence, the two neutron emission processes from the compound nucleus of  ${}^{11}\text{B}$  belong to the  $(n, 2np)2\alpha$  reaction channel.

For the residual nucleus  ${}^9\text{Be}$  produced by  $(n, np)$  and  $(n, pn)$  emission processes, as is well known, the ground state of  ${}^9\text{Be}$  is stable. In this case the reaction is the  $(n, np) {}^9\text{Be}_g$  channel, while the excited levels of  ${}^9\text{Be}$  can emit neutron or  $\alpha$ -particle and become one neutron and two  $\alpha$ -particles, so the reactions also belong to  $(n, 2np)2\alpha$  channel.

The residual nucleus  ${}^6\text{Li}$  is from  $(n, n\alpha)$  and  $(n, \alpha n)$  emission processes. As indicated in Ref. [4], the ground state of  ${}^6\text{Li}$  is stable, and the second excited level of  ${}^6\text{Li}$  only decays through gamma de-excitation to its ground state, so they are the  $(n, n\alpha) {}^6\text{Li}_g$  reaction channel, while the other excited levels of  ${}^6\text{Li}$  can issue the two-body breakup into one deuteron and one  $\alpha$ -particle, and belong to the  $(n, nd)2\alpha$  reaction channel.

The residual nucleus  ${}^8\text{Be}$  is produced by  $(n, nd)$  and  $(n, dn)$  emission processes.  ${}^8\text{Be}$  is unstable and separated into two  $\alpha$ -particles spontaneously, which also belongs to the  $(n, nd)2\alpha$  reaction channel.

The residual nucleus  ${}^6\text{He}$  is produced by  $(n, \alpha p)$  emission processes. The ground state of  ${}^6\text{He}$  is unstable via beta decay and contributes to the  $(n, \alpha p) {}^6\text{He}_g$  reaction channel, while the first excited state has the energy of 1.797 MeV, which is below the neutron binding energy, so it only decays through three-body break-up process ( ${}^6\text{He} \rightarrow n + n + \alpha$ ) and contributes to  $(n, 2np)2\alpha$  channel.

The reaction channel of  $(n, {}^3\text{He})$  is not open due to the threshold energy over 14.2 MeV, while the reaction channel of  $(n, {}^5\text{He})$  is opened with the threshold energy of 5.8944 MeV.  ${}^5\text{He}$  is unstable and separated into  $n + \alpha$  spontaneously. The residual nucleus is  ${}^6\text{Li}$ , as mentioned above, the ground state and the second excited state of  ${}^6\text{Li}$  reached by  ${}^5\text{He}$  emission belong to the  $(n, n\alpha) {}^6\text{Li}$  reaction channel, otherwise belong to  $(n, nd)2\alpha$  reaction channel.

Besides the partial reaction channels listed in Table 1, there are also other reaction channels, such as  $(n, \alpha) {}^7\text{Li}^*$ ,  $(n, p) {}^{10}\text{Be}^*$ ,  $(n, \alpha) {}^7\text{Li}_g$ ,  $(n, d) {}^9\text{Be}_g$ , and  $(n, t)2\alpha$ , which are not listed in this table due to no outgoing neutrons. The reaction channel of  $(n, \alpha)$  is caused by  $\alpha$ -particle emissions to the ground state and the first excited levels of  ${}^7\text{Li}$ , which decay through gamma de-excitation to its ground state. The  $(n, p)$  reaction channel is yielded by a proton emission, all of the excited levels are below the 5-th excited

levels of the residual nucleus  ${}^{10}\text{Be}^*$  and decay through the gamma de-excitation into its ground state, which has the  $\beta$ -decay further, while above the 5-th excited levels can emit a neutron and reach to the ground state of  ${}^9\text{Be}$ , which belongs to the  $(n, np) {}^9\text{Be}$  reaction channel. The reaction channel  $(n, d)$  is from the emission of deuteron from the compound nucleus of  ${}^{11}\text{B}$  to the ground state of  ${}^9\text{Be}$ . The reaction channels leading to one triton and two  $\alpha$ -particles may proceed via different ways to  $(n, t)2\alpha$  channel as follows:

- (i)  ${}^{10}\text{B}(n, t) {}^8\text{Be}$ , and  ${}^8\text{Be} \rightarrow \alpha + \alpha$ ,
- (ii)  ${}^{10}\text{B}(n, \alpha) {}^7\text{Li}^*$  and  ${}^7\text{Li}^* \rightarrow t + \alpha$ .

A large number of discrete levels are listed in Table 1, all of which are needed in the model calculation. The discrete schemes, including the individual level energy, spin and parity used for every reaction channel, are taken from the Table of Isotopes 8-th.<sup>[5]</sup>

In the case of  $n+{}^{10}\text{B}$ , the reaction situation from the compound nucleus  ${}^{11}\text{B}^*$  to the discrete levels of the residual nuclei including the outgoing neutrons at  $E_n = 14.2$  MeV is presented in Table 1.

**Table 1** The reaction situation from the compound nucleus  ${}^{11}\text{B}^*$  to open the  $k_2$  level of the residual nucleus via the  $k_1$  level for variety reactions at  $E_n = 14.2$  MeV.

Channel	$k_1$	$k_2$	R.N
$(n, 2n)$	22–25	<i>g.s</i>	${}^9\text{B}$
$(n, 2n)$	26	<i>g.s -2</i>	${}^9\text{B}$
$(n, 2n)$	27–28	<i>g.s -3</i>	${}^9\text{B}$
$(n, np)$	13–21	<i>g.s</i>	${}^9\text{Be}$
$(n, np)$	22–24	<i>g.s -1</i>	${}^9\text{Be}$
$(n, np)$	25–26	<i>g.s -4</i>	${}^9\text{Be}$
$(n, np)$	27–28	<i>g.s -5</i>	${}^9\text{Be}$
$(n, n\alpha)$	6–12	<i>g.s</i>	${}^6\text{Li}$
$(n, n\alpha)$	13–21	<i>g.s -1</i>	${}^6\text{Li}$
$(n, n\alpha)$	22–24	<i>g.s -2</i>	${}^6\text{Li}$
$(n, n\alpha)$	25	<i>g.s -3</i>	${}^6\text{Li}$
$(n, n\alpha)$	26–28	<i>g.s -5</i>	${}^6\text{Li}$
$(n, nd)$	11–24	<i>g.s</i>	${}^8\text{Be}$
$(n, nd)$	25–28	<i>g.s -1</i>	${}^8\text{Be}$
$(n, pn)$	6	<i>g.s</i>	${}^9\text{Be}$
$(n, \alpha n)$	4	<i>gs</i>	${}^6\text{Li}$
$(n, \alpha n)$	5–6	<i>g.s -1</i>	${}^6\text{Li}$
$(n, \alpha n)$	7	<i>g.s -2</i>	${}^6\text{Li}$
$(n, \alpha n)$	8–9	<i>g.s -5</i>	${}^6\text{Li}$
$(n, \alpha p)$	7	<i>gs</i>	${}^6\text{He}$
$(n, \alpha p)$	8–9	<i>g.s -1</i>	${}^6\text{He}$
$(n, {}^5\text{He})$	<i>g.s -5</i>		${}^6\text{Li}$
$(n, dn)$	1–5	<i>g.s</i>	${}^8\text{Be}$
$(n, dn)$	6–7	<i>g.s -1</i>	${}^8\text{Be}$

The acronym  $k_1$  and  $k_2$  refer to the order number of the excited levels in the corresponding reaction channel.

The acronym g.s. stands for the ground state (same as in Table 2). The acronym R.N stands for the residual nucleus.

From Table 1 one can see that the first five excited levels of  $^{10}\text{B}$  purely belong to the inelastic scattering reaction.

### 3 Classification of the Reaction Mechanism

The reaction mechanism of neutron induced  $^{10}\text{B}$  is the most complex one in 1P-shell nuclei. The number of the opened partial reaction channels is over one hundred even at  $E_n = 14.2$  MeV.

The total neutron energy-angular spectra consist of the outgoing neutrons from various reaction channels and different discrete levels, which strongly differ from each other in their respective energy-angular distributions. The double-differential cross sections can provide information for analysis the components from the differential reaction mechanism. The research indicates that the kinematics of various secondary particle emission processes can be classified into the following four possible types in variety of light nucleus reactions.

- (i) From discrete level to discrete level (D to D);
- (ii) From continuum spectrum to discrete level (C to D);
- (iii) From discrete level to continuum spectrum (D to C);
- (iv) From continuum spectrum to continuum spectrum (C to C).

The first two terms are used in the sequential particle emissions, because their final states are discrete levels; while the last two terms are used for three-body breakup processes, due to their final states being in the form of continuum spectra. All of the representation of the double-differential cross sections of the outgoing particles with the energy balance for various emission processes has been obtained analytically. One can find them in Refs. [1], [2], [4], [6], and [7], so in this paper we do no longer repeat the representations.

The first emitted neutrons and charged particles listed in Table 1 have definite energies in CMS. The energy-angular spectra of the second emitted particles listed in Table 1 can be presented by the formula of D to D.<sup>[1]</sup> In the  $^5\text{He}$  emission process, the neutron energy-angular spectra can also be treated as the sequential particle emission, only that the binding energy of the neutron in  $^5\text{He}$  is negative. The outgoing neutron energy-angular spectra can also be presented by the formula of D to D.

Particularly, for the  $(n, \alpha p)$  reaction channel, the residual nucleus  $^6\text{He}^*$  undergoes the three-body breakup process, from which the outgoing neutron energy-angular spectra should be presented by the formula of C to C, because the three-body breakup process is from the ring-type spectra of the outgoing proton. In addition, all of

the particles emitted from the residual nuclei after two particle sequential emissions, the double-differential cross sections should be presented by the formula of C to D.

### 4 Calculated Results and Discussions

The LUNF code of  $n+^{10}\text{B}$  reaction is developed for calculating the cross sections and the double-differential cross sections of outgoing neutrons and charged particles of each reaction channel below 20 MeV.

The calculations of the double-differential cross sections of the total outgoing neutrons from each reaction channels have been performed. The comparisons of the calculated results with the measured data are shown in Figs. 1 ~ 10 at the incident neutron energy  $E_n = 14.2$  MeV for outgoing angles of  $25^\circ$ ,  $30^\circ$ ,  $45^\circ$ ,  $60^\circ$ ,  $75^\circ$ ,  $85^\circ$ ,  $100^\circ$ ,  $120^\circ$ ,  $135^\circ$ , and  $150^\circ$ , respectively. The fittings agree fairly well with the measurements. The measured data are taken from Ref. [3].

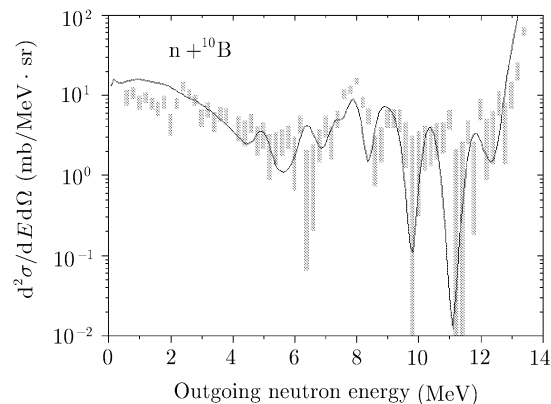


**Fig. 1** The energy-angular spectra of  $25^\circ$  at  $E_n = 14.2$  MeV.

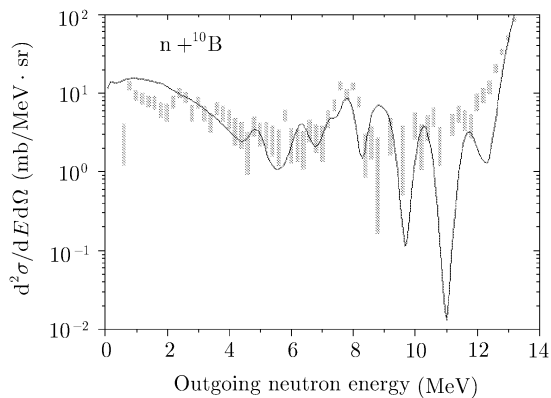


**Fig. 2** The energy-angular spectra of  $30^\circ$  at  $E_n = 14.2$  MeV.

In the  $n+^{10}\text{Be}$  reactions, the pre-equilibrium emission process is the dominating reaction mechanism, which is the same as other light nuclei, like lithium,<sup>[4,7]</sup> carbon,<sup>[1]</sup> as well as oxygen.<sup>[2]</sup> The percentage of pre-equilibrium emission is 70.99%, while percentage of equilibrium is only

29.01% in  $n+^{10}\text{B}$  reactions at  $E_n = 14.2$  MeV. Thus, the equilibrium theory, like Hauser–Feshbach model, cannot work on the light nucleus reaction.

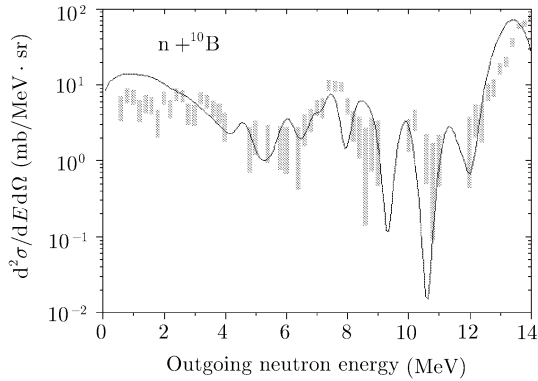


**Fig. 3** The energy-angular spectra of  $45^\circ$  at  $E_n = 14.2$  MeV.

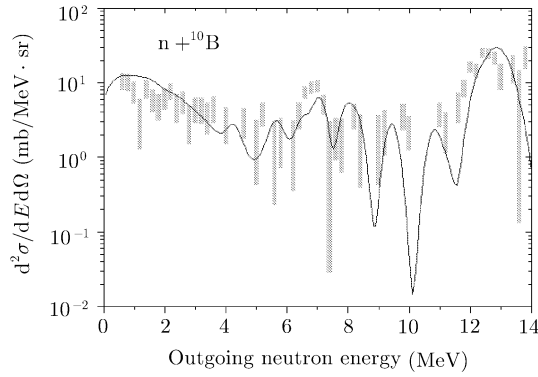


**Fig. 4** The energy-angular spectra of  $60^\circ$  at  $E_n = 14.2$  MeV.

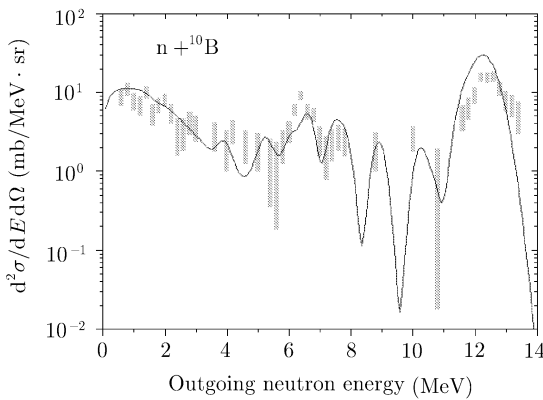


**Fig. 5** The energy-angular spectra of  $75^\circ$  at  $E_n = 14.2$  MeV.

The total energy-angular spectrum for each angle consists of many partial spectra from differential reaction channels. As an example, the case for  $\theta = 85^\circ$  at  $E_n = 14.2$  MeV is shown in Fig. 11. In the case of  $n+^{10}\text{B}$ , it is very difficult to specify the partial spectra with the designations in one figure. From Table 2, one can see that

each total energy-angular spectrum consists of about 90 curves at  $E_n = 14.2$  MeV. So only the elastic scattering peak with the designation  $e_l$  and the first four excited levels of  $^{10}\text{B}$  with the designations 1, 2, 3, 4, respectively, as the inelastic scattering channels given in Fig. 11.

The calculated cross sections related to the neutron emissions are shown in Table 2 at  $E_n = 14.2$  MeV. The cross sections that are smaller than 0.01 mb are not included in this table.

**Table 2** The calculated partial cross sections of the inelastic scattering and the variety partial reaction channels to the  $k_2$  level of the residual nucleus via the  $k_1$  level at  $E_n = 14.2$  MeV.

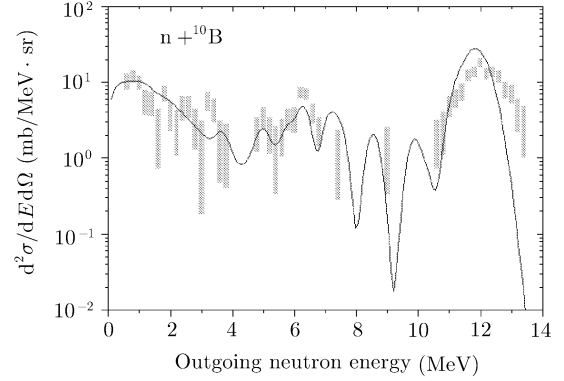
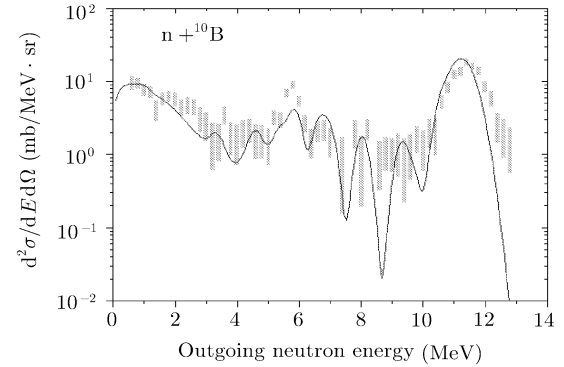
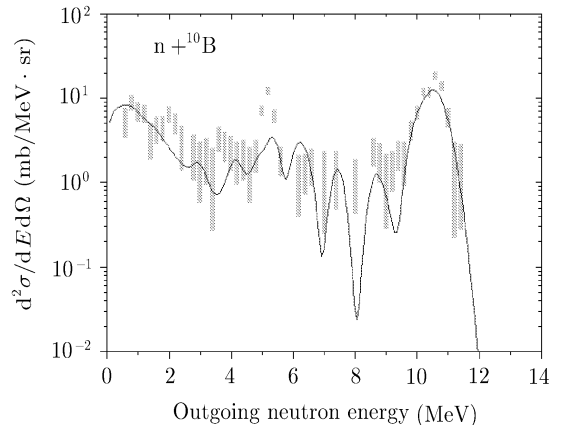
	$E_{\text{th}}$	$k_1$	$k_2$	$\sigma$ (mb)	Channel
$(n, n)$	0.791	1		19.89	$(n, n)$
$(n, n)$	1.915	2		4.33	$(n, n)$
$(n, n)$	2.371	3		12.67	$(n, n)$
$(n, n)$	3.949	4		16.27	$(n, n)$
$(n, n)$	5.255	5		19.31	$(n, n)$
$(n, 2n)$	9.784	23	<i>g.s.</i>	0.22	$(n, 2np)2\alpha$
$(n, 2n)$	9.790	24	<i>g.s.</i>	0.22	$(n, 2np)2\alpha$
$(n, 2n)$	11.93	26	<i>g.s.</i>	0.14	$(n, 2np)2\alpha$
$(n, 2n)$	11.93	26	1	0.01	$(n, 2np)2\alpha$
$(n, 2n)$	12.68	27	1	0.20	$(n, 2np)2\alpha$
$(n, np)$	7.566	13	<i>g.s.</i>	0.11	$(n, np)^9\text{Be}$
$(n, np)$	8.178	15	<i>g.s.</i>	1.21	$(n, np)^9\text{Be}$
$(n, np)$	8.219	16	<i>g.s.</i>	0.23	$(n, np)^9\text{Be}$
$(n, np)$	8.231	17	<i>g.s.</i>	1.82	$(n, np)^9\text{Be}$
$(n, np)$	8.321	18	<i>g.s.</i>	0.78	$(n, np)^9\text{Be}$
$(n, np)$	8.443	19	<i>g.s.</i>	0.31	$(n, np)^9\text{Be}$
$(n, np)$	8.607	20	<i>g.s.</i>	0.68	$(n, np)^9\text{Be}$
$(n, np)$	8.883	21	<i>g.s.</i>	1.92	$(n, np)^9\text{Be}$
$(n, np)$	9.576	22	<i>g.s.</i>	0.40	$(n, np)^9\text{Be}$
$(n, np)$	9.784	23	<i>g.s.</i>	0.88	$(n, np)^9\text{Be}$
$(n, np)$	9.790	24	<i>g.s.</i>	1.42	$(n, np)^9\text{Be}$
$(n, np)$	10.68	25	<i>g.s.</i>	0.25	$(n, np)^9\text{Be}$
$(n, np)$	10.68	25	1	0.15	$(n, 2np)2\alpha$
$(n, np)$	11.92	26	<i>g.s.</i>	0.30	$(n, np)^9\text{Be}$
$(n, np)$	11.92	26	2	0.12	$(n, 2np)2\alpha$
$(n, np)$	11.92	26	4	0.12	$(n, 2np)2\alpha$
$(n, np)$	12.68	27	<i>g.s.</i>	0.20	$(n, np)^9\text{Be}$
$(n, np)$	12.68	27	2	0.20	$(n, 2np)2\alpha$
$(n, np)$	12.68	27	4	0.19	$(n, 2np)2\alpha$
$(n, n\alpha)$	5.625	6	<i>g.s.</i>	10.42	$(n, n\alpha)^6\text{Li}$
$(n, n\alpha)$	5.684	7	<i>g.s.</i>	10.21	$(n, n\alpha)^6\text{Li}$
$(n, n\alpha)$	5.702	8	<i>g.s.</i>	5.13	$(n, n\alpha)^6\text{Li}$
$(n, n\alpha)$	6.516	9	<i>g.s.</i>	8.24	$(n, n\alpha)^6\text{Li}$
$(n, n\alpha)$	6.632	10	<i>g.s.</i>	18.54	$(n, n\alpha)^6\text{Li}$
$(n, n\alpha)$	6.744	11	<i>g.s.</i>	13.09	$(n, n\alpha)^6\text{Li}$
$(n, n\alpha)$	7.221	12	<i>g.s.</i>	17.65	$(n, n\alpha)^6\text{Li}$
$(n, n\alpha)$	7.566	13	<i>g.s.</i>	2.31	$(n, n\alpha)^6\text{Li}$
$(n, n\alpha)$	7.708	14	<i>g.s.</i>	3.03	$(n, n\alpha)^6\text{Li}$
$(n, n\alpha)$	8.178	15	<i>g.s.</i>	2.55	$(n, n\alpha)^6\text{Li}$

**Table 2** (Continued).

$(n, n\alpha)$	8.219	16	g.s	0.93	$(n, n\alpha)^6\text{Li}$
$(n, n\alpha)$	8.231	17	g.s	1.85	$(n, n\alpha)^6\text{Li}$
$(n, n\alpha)$	8.443	19	g.s	0.82	$(n, n\alpha)^6\text{Li}$
$(n, n\alpha)$	8.607	20	g.s	0.99	$(n, n\alpha)^6\text{Li}$
$(n, n\alpha)$	8.883	21	g.s	0.99	$(n, n\alpha)^6\text{Li}$
$(n, n\alpha)$	9.576	22	g.s	0.44	$(n, n\alpha)^6\text{Li}$
$(n, n\alpha)$	9.784	23	g.s	1.26	$(n, n\alpha)^6\text{Li}$
$(n, n\alpha)$	9.784	23	1	2.48	$(n, n\alpha)2\alpha$
$(n, n\alpha)$	9.790	24	g.s	0.53	$(n, n\alpha)^6\text{Li}$
$(n, n\alpha)$	9.790	24	1	0.11	$(n, nd)2\alpha$
$(n, n\alpha)$	10.68	25	g.s	0.21	$(n, n\alpha)^6\text{Li}$
$(n, n\alpha)$	12.68	27	g.s	0.12	$(n, n\alpha)^6\text{Li}$
$(n, n\alpha)$	12.68	27	1	0.20	$(n, n\alpha)^6\text{Li}$
<hr/>					
$(n, nd)$	7.221	12	g.s	0.18	$(n, nd)2\alpha$
$(n, nd)$	7.556	13	g.s	0.81	$(n, nd)2\alpha$
$(n, nd)$	7.708	14	g.s	1.74	$(n, nd)2\alpha$
$(n, nd)$	8.178	15	g.s	1.74	$(n, nd)2\alpha$
$(n, nd)$	8.219	16	g.s	1.54	$(n, nd)2\alpha$
$(n, nd)$	8.231	17	g.s	1.68	$(n, nd)2\alpha$
$(n, nd)$	8.321	18	g.s	1.42	$(n, nd)2\alpha$
$(n, nd)$	8.607	20	g.s	0.81	$(n, nd)2\alpha$
$(n, nd)$	8.883	21	g.s	1.52	$(n, nd)2\alpha$
$(n, nd)$	9.576	22	g.s	0.85	$(n, nd)2\alpha$
$(n, nd)$	9.784	23	g.s	0.78	$(n, nd)2\alpha$
$(n, nd)$	9.790	24	g.s	1.05	$(n, nd)2\alpha$
$(n, nd)$	10.67	25	g.s	0.40	$(n, nd)2\alpha$
$(n, nd)$	11.93	26	g.s	0.19	$(n, nd)2\alpha$
$(n, nd)$	11.93	26	1	0.50	$(n, nd)2\alpha$
$(n, nd)$	12.68	27	g.s	0.26	$(n, nd)2\alpha$
$(n, nd)$	12.68	27	1	0.54	$(n, nd)2\alpha$
<hr/>					
$(n, \alpha n)$	5.140	4	g.s	2.66	$(n, n\alpha)^6\text{Li}$
$(n, \alpha n)$	7.573	5	1	2.13	$(n, nd)2\alpha$
$(n, \alpha n)$	7.771	6	g.s	1.08	$(n, n\alpha)^6\text{Li}$
$(n, \alpha n)$	7.771	6	1	0.12	$(n, nd)2\alpha$
$(n, \alpha n)$	9.301	7	g.s	0.50	$(n, n\alpha)^6\text{Li}$
$(n, \alpha n)$	9.301	7	1	0.16	$(n, nd)2\alpha$
<hr/>					
$(n, \alpha p)$	9.301	7	g.s	0.15	$(n, \alpha p)^6\text{He}$
<hr/>					
$(n, dn)$	6.656	1	g.s	18.71	$(n, nd)2\alpha$
$(n, dn)$	7.476	2	g.s	51.57	$(n, nd)2\alpha$
$(n, dn)$	7.861	3	g.s	13.31	$(n, nd)2\alpha$
$(n, dn)$	8.158	4	g.s	44.56	$(n, nd)2\alpha$
$(n, dn)$	9.979	5	g.s	14.79	$(n, nd)2\alpha$
$(n, dn)$	12.24	6	g.s	0.25	$(n, nd)2\alpha$
$(n, dn)$	12.24	6	1	12.83	$(n, nd)2\alpha$
$(n, dn)$	13.54	7	g.s	0.14	$(n, nd)2\alpha$
<hr/>					
$(n, ^5\text{He})$	5.894	g.s		12.47	$(n, n\alpha)^6\text{Li}$
$(n, ^5\text{He})$	8.301	1		26.03	$(n, nd)2\alpha$
$(n, ^5\text{He})$	9.816	2		0.94	$(n, n\alpha)^6\text{Li}$
$(n, ^5\text{He})$	10.64	3		4.07	$(n, nd)2\alpha$
$(n, ^5\text{He})$	11.80	4		2.98	$(n, nd)2\alpha$
$(n, ^5\text{He})$	12.11	5		1.08	$(n, nd)2\alpha$

At  $E_n = 14.2$  MeV, the contributions from variety of reaction channels are mainly from the  $(n, nd)2\alpha$  and  $(n, n\alpha)^6\text{Li}$  channels with the cross sections of 212 mb and

115 mb, respectively, while the other channels, such as  $(n, 2np)2\alpha$ ,  $(n, np)$ , and  $(n, \alpha p)$  only have the values of the reaction cross sections of 2.2 mb, 17.9 mb, and 0.2 mb, respectively. The results indicate that the partial cross section of the reaction channel through  $(n, \alpha p)$  emissions to the first excited level of  $^6\text{He}$  is so small that it can be neglected. Therefore, the three-body breakup mechanism does not give obvious contribution at  $E_n = 14.2$  MeV, which becomes important at high neutron incident energies.

**Fig. 6** The energy-angular spectra of  $85^\circ$  at  $E_n = 14.2$  MeV.**Fig. 7** The energy-angular spectra of  $100^\circ$  at  $E_n = 14.2$  MeV.**Fig. 8** The energy-angular spectra of  $120^\circ$  at  $E_n = 14.2$  MeV.

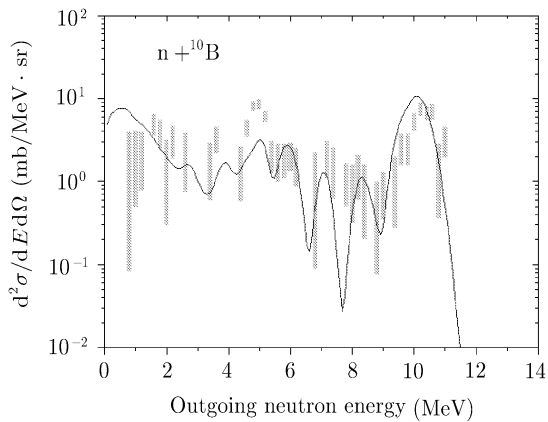


**Fig. 9** The energy-angular spectra of  $135^\circ$  at  $E_n = 14.2$  MeV.

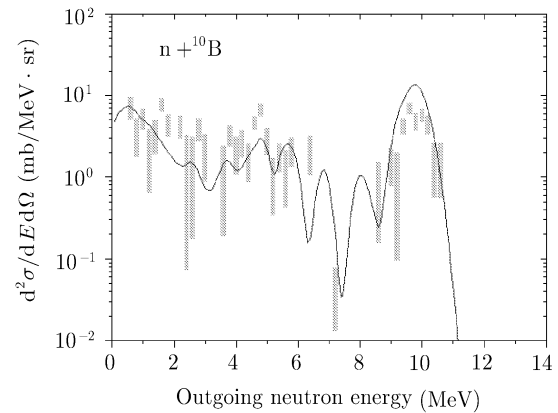


**Fig. 10** The energy-angular spectra of  $150^\circ$  at  $E_n = 14.2$  MeV.

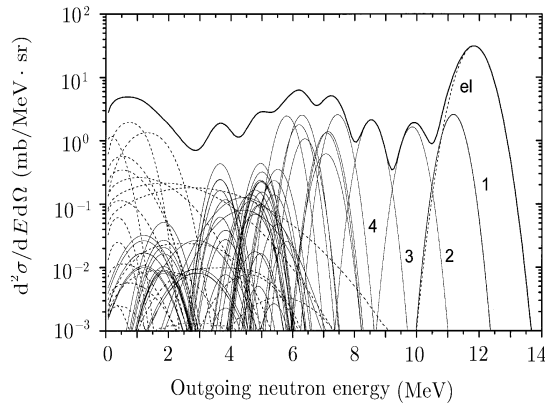


**Fig. 11** The partial energy-angular spectra of  $85^\circ$  at  $E_n = 14.2$  MeV. The solid line is the calculated total neutron energy-angular spectrum, and the dashed lines correspond to the outgoing neutron spectra from energy partial reaction channels listed in Table 2.

## 5 Summary

The model for neutron induced light nucleus reaction

has been proposed. In this model, the particle emission from the compound nucleus to discrete levels in pre-equilibrium mechanism is taken into account with the angular momentum conservation. The pre-equilibrium reaction mechanism plays an important role for the description of the reaction cross sections and the double-differential cross sections. On the other hand, the accurate kinematics also plays an important role in the light nucleus reactions, since the recoil effect of the particle emissions is very strong.

Then the double-differential cross sections have been calculated to fitting the measured data from lithium to oxygen. The entire fitting agrees fairly well with the measurement, which implies that this new approach has the ability to analyze the experimental data for light nucleus reactions. Meanwhile, the accurate kinematics used in this model for the various reactions mechanism not only gives the correct spectrum shape of the outgoing particles, but also provides the method to set up file-6 for double-differential cross sections in neutron data library with full energy balance.

## References

- [1] J.S. Zhang, Y.L. Han, and L.G. Cao, Nucl. Sci. Eng. **133** (1999) 218.
- [2] J.S. Zhang, *et al.*, Commun. Theor. Phys. (Beijing, China) **35** (2001) 579.
- [3] M. Baba, *et al.*, "Scattering of 14.2 MeV Neutrons from B-10, B-11, C, N, O, F and SI, C", 85 Santa **1** (1985) 223.
- [4] J.S. Zhang and Y.L. Han, Commun. Theor. Phys. (Beijing, China) **36** (2001) 437.
- [5] R.B. Firestone and V.S. Shirley, *Table of Isotopes 8th*, John Wiley & Sons (1996).
- [6] J.S. Zhang, Commun. Theor. Phys. (Beijing, China) **39** (2003) 83.
- [7] J.S. Zhang and Y.L. Han., Commun. Theor. Phys. (Beijing, China) **37** (2001) 465.